

# Planting of bis(1,5-cyclooctadiene) nickel upon silica to harvest NiO (<5 nm) nanoparticles in a silica matrix

Kake Zhu, Lawrence D'Souza and Ryan M. Richards\*

School of Engineering and Science, International University of Bremen, 28759 Bremen, Germany

Received 6 June 2005; Accepted 20 June 2005

Bis(1,5-cyclooctadiene) nickel [Ni(COD)<sub>2</sub>] was employed as a nickel precursor to prepare nickel oxide nanoparticles upon high-surface-area mesoporous silica. Under protection of argon, Ni(COD)<sub>2</sub> was dissolved in tetrahydrofuran (THF) to react with surface silanols of mesoporous silica SBA-15, which formed a black powder after completion of the surface reaction. Calcination of the powder produced ultrafine NiO inside the mesoporous silica matrix, which was evidenced by X-ray diffraction, N<sub>2</sub> adsorption–desorption, transmission electron microscopy and thermogravimetric analysis. The thermogravimetric analysis suggests that NiO formation is a result of surface nickel species calcination, whereas structural characterization clearly show that NiO nanoparticles of <5 nm are evenly distributed inside the silica SBA-15 matrix and mesoporosity is well preserved upon calcinations and NiO formation. The surface reaction between Ni(COD)<sub>2</sub> and surface silanols was found for the first time, and the method used here may be extended conveniently to prepare other metal oxide nanoparticles upon high-surface-area supports as well. Copyright © 2005 John Wiley & Sons, Ltd.

**KEYWORDS:** bis(1,5-cyclooctadiene) nickel; mesoporous silica; NiO; nanoparticle; grafting; surface modification

## INTRODUCTION

Heterogeneous catalysis relies on the understanding of structure–activity relationships, but it is much easier to disperse metal oxides on a high-surface-area support than to tailor the surface chemistry precisely, which becomes even more difficult when nanoparticle sizes of <5 nm are involved.<sup>1</sup> The conventionally employed aqueous impregnation method usually results in uneven dispersion and poor particle size distribution with aggregation of metal centres during the drying process, which is caused by the weak interaction between support and precursor.<sup>2</sup> Chemical vapour deposition and grafting methods have been found to be efficient in improving the dispersion through the reaction between the precursor and the support surface hydroxyl groups. Atomically dispersed isolated Ti,<sup>3</sup> V,<sup>4</sup> Fe,<sup>5</sup> Cu,<sup>6</sup> Ta,<sup>7</sup> Cr and W centres<sup>8</sup> have been synthesized through grafting of either organometallics or metal-containing silsequioxane species in organic solvents and, as a result, catalytic activity

can be related directly to the well-characterized surface structure. Ultrafine nanoparticles upon porous support have been achieved by similar methods: Ti,<sup>9</sup> Ga,<sup>10</sup> Mg,<sup>11</sup> Al,<sup>11</sup> Cr<sup>12</sup> and Fe<sup>13</sup> silsequioxanes form highly dispersed nanoparticles upon microporous silica after air calcination, during which the strong bonding between metal centres and silsequioxanes stops the aggregation of metal species and therefore improves the dispersion of metal species. It is noteworthy to mention that most of these materials are superior in catalytic properties to those prepared by conventional wet impregnation methods, because the essence of a better dispersion is the strong interaction between the precursor and support. Here, we present a grafting method to synthesize well-dispersed NiO nanoparticles upon high-surface-area mesoporous silica by using bis(1,5-cyclooctadiene) nickel [Ni(COD)<sub>2</sub>] as a precursor under mild conditions in tetrahydrofuran (THF). Because metals such as copper, ruthenium, etc. form similar compounds, extension of the present method to these systems may be possible as well.

The Ni(COD)<sub>2</sub> was once reported to synthesize nickel metal particles in a sol–gel process by reacting with functional Si–H organic groups, in which the cyclooctadiene groups are reduced during formation of nickel particles<sup>14</sup> by the

\*Correspondence to: Ryan M. Richards, School of Engineering and Science, International University of Bremen, 28759 Bremen, Germany. E-mail: r.richards@iu-bremen.de  
Contract/grant sponsor: International University of Bremen.

functional organic groups. We found that  $\text{Ni}(\text{COD})_2$  can react directly with surface silanols under anhydrous conditions for the first time, however no reaction was observed in the presence of water or with the undried mesoporous silica. It is thus suspected that this 'sensitivity' to the presence of water may be the 'hidden' reason why  $\text{Ni}(\text{COD})_2$  was never used to graft upon supports. Moreover,  $\text{Ni}(\text{COD})_2$  is found to be quite stable in the presence of water, even resistant to hydrogen flush treatment, which suggests that  $\text{Ni}(\text{COD})_2$  interacts very differently in anhydrous solvents. No parallel work has been reported to the best of our knowledge.

The nickel/silica system is very useful in either its oxidized or reduced metal form. Applications can be found in heterogeneous catalysis for various hydrogenation processes and the decomposition of hypochloride,<sup>15</sup> or as hydrogen storage materials.<sup>16</sup> The chemical route to prepare such a material generally involves dispersion of a salt upon silica (wet impregnation, ion-exchange or deposition-precipitation) and a subsequent reduction of the salt to the metallic state, however the various preparation procedures can produce materials with very different characteristics, morphologies and catalytic activities. Many efforts have been exerted to explore the preparation methods: Che and co-workers explored the interaction between nickel complexes and silica as a function of the preparation procedure<sup>17</sup> and developed a two-step procedure to control the surface chemistry and particle size of nickel in the system;<sup>18</sup> Boudjahem *et al.* studied the use of hydrazine to reduce the nickel acetate upon silica;<sup>16</sup> and Casula *et al.*<sup>19</sup> explored the formation of nickel silica aerogels and xerogels in supercritical ethanol. These studies demonstrated the complexity of the system and the difficulties in controlling the species upon silica. There is still no convenient way to achieve the tailoring of the surface chemistry, nor has any improved methodology to synthesize nickel nanoparticles upon silica been elaborated to date.

Mesoporous silica SBA-15<sup>20</sup> is chosen as the support due to its high surface area, regular mesopores with larger pore diameter (compared with MCM-41), three-dimensional pore systems and large pore volumes, which facilitates mass transfer for the metal precursors and substrates in catalytic reactions.

## EXPERIMENTAL

### Materials and sample preparation

Mesoporous silica SBA-15 was synthesized in acidic conditions using the tri-block copolymer poly(ethylene oxide)-poly(propylene oxide)-poly(ethylene oxide) P123, ( $\text{EO}_{20}\text{PO}_{70}\text{EO}_{20}$ , BASF) as template and tetraethyl orthosilicate (TEOS, 98%, Aldrich) as a silicon source. A solution of P123-2M HCl-TEOS- $\text{H}_2\text{O}$  with a mass ratio of 2 : 60 : 4.25 : 15 was prepared, stirred for 24 h at 40 °C and then heated at 95 °C in an autoclave for 3 days. The solid products were filtered and calcinated at 550 °C for 5 h to remove the polymer

template by combustion. A 1.0 g quantity of white powder was transferred to a Schlenk tube to remove surface water under vacuum by heating to 180 °C for 8 h. Then 0.10 g of  $\text{Ni}(\text{COD})_2$  was dissolved in THF in a three-necked flask with stirring under argon gas protection and the solution was injected into the Schlenk tube by syringe. The SBA-15 and  $\text{Ni}(\text{COD})_2$  solution was stirred for 12 h; the yellowish solvent became colourless and the powder became yellow during the first 2–3 h and then the powder changed to black as the reaction between  $\text{Ni}(\text{COD})_2$  and surface silanols proceeded, until finally a black powder and a transparent clear solution were observed. After filtration, the black powder was collected and calcinated in air at 773 K for 5 h.

Small- and wide-angle X-ray diffractograms were recorded on a Siemens D5000 diffractometer using  $\text{Cu K}\alpha$  ( $\lambda = 0.15406$  nm, 40 kV, 40 mA) as a radiation light source, starting from 0.5° to 10° and 20° to 60° respectively at a scanning speed of 0.06° min<sup>-1</sup>. Thermogravimetric and differential thermal analysis (TG-DTA) was made using SDT Q600 instruments in air at a ramp rate of 3 °C min<sup>-1</sup> from room temperature to 1000 °C. Nitrogen adsorption-desorption isotherms at -196 °C were obtained with a Quantachrome Autosorb 1-C system, and the data were analysed by employing the BJH (Barrett-Joyner-Halenda) method; pore volume and pore size distribution curves are from the desorption branch of the isotherm. High-resolution transmission electron microscopy images were obtained with a JEOL 200CX electron microscope operating at 200 kV.

## RESULTS AND DISCUSSION

The TG-DTA of  $\text{Ni}(\text{COD})_2$  grafted to SBA-15 is shown in Fig. 1, which displays two major weight losses from room

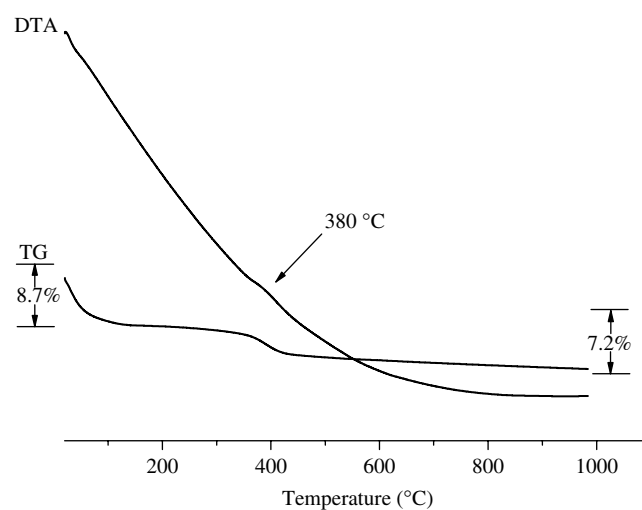


**Figure 1.** The TG-DTA of  $\text{Ni}(\text{COD})_2$  grafted on SBA-15 in air at a ramp rate of 3 °C min<sup>-1</sup>: *in situ* formation of NiO from grafted nickel species occurs at 380 °C.

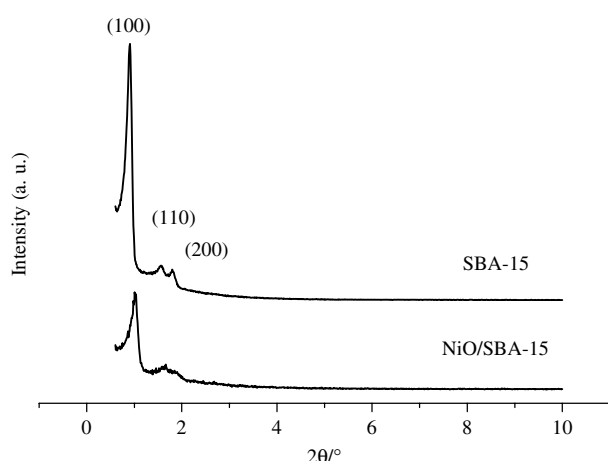


**Figure 2.** Small-angle X-ray diffraction of SBA-15 and NiO/SBA-15.

temperature to 1000 °C. The first weight loss of 8.7% begins from room temperature to 120 °C and is attributed to the loss of physically adsorbed water or THF in the sample, because there is no thermal change that can be identified from the corresponding DTA curve. The second weight loss of 7.2% is observed from 350 to 400 °C and is caused by the combustion of grafted nickel species, as evidenced by the small exothermic peak in the DTA curve at ~380 °C. The NiO formation can hardly be identified from either peak, suggesting that NiO was also formed during the second weight loss; this also indicates that the Ni(COD)<sub>2</sub> species has chemically interacted with the surface silanols.

Small-angle X-ray diffractograms of pure silica SBA-15 and NiO/SBA-15 are shown in Fig. 2. Both samples exhibit three peaks that can be indexed to (100), (110) and (200) reflections of the two-dimensional hexagonal structure (*P6m*) characteristic of SBA-15, indicating that the host structure of

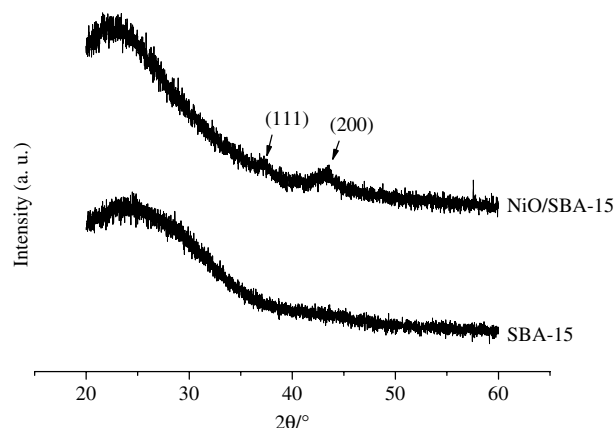


**Figure 3.** Wide-angle X-ray diffraction of NiO/SBA-15.

the well-ordered mesoporous silica is well preserved after the formation of NiO inside its matrix. The slight decrease in peak intensity can be attributed to the partial pore filling of the mesopores caused by NiO formation within the pore systems. The minor shift of reflection peaks of NiO/SBA-15 to high angles compared with SBA-15 accounts for the host framework contraction during NiO formation upon calcination. Wide-angle X-ray diffractograms of both samples are shown in Fig. 3. In the case of SBA-15, only one broad peak from amorphous silica observed from 20° to 30° can be identified, whereas in the NiO/SBA-15 sample two small peaks corresponding to NiO (JCPDS 78-0429) (111) and (200) reflections can be identified. A particle size of  $3.6 \pm 1.5$  nm can be deduced by application of the Scherrer equation from the latter reflection.

Nitrogen adsorption–desorption isotherms of both samples show a typical type IV isotherm and a hysteresis loop (Fig. 4) characteristic of mesoporous systems. The NiO/SBA-15 sample retains the same isotherm shape but

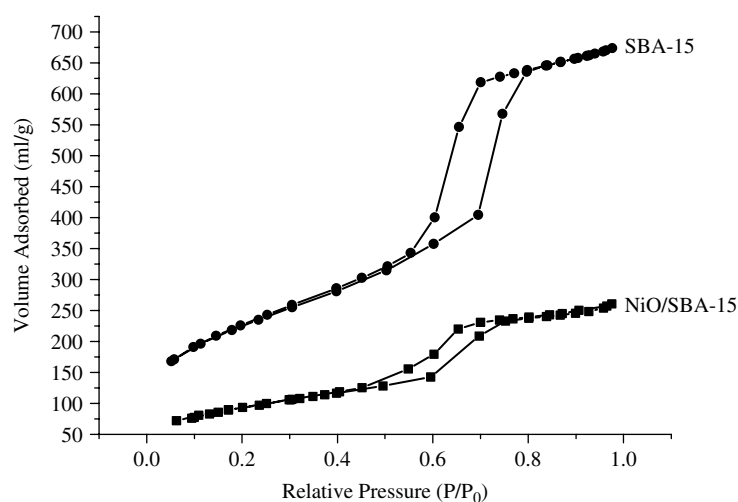


**Figure 4.** Nitrogen adsorption–desorption curve of SBA-15 and NiO/SBA-15.

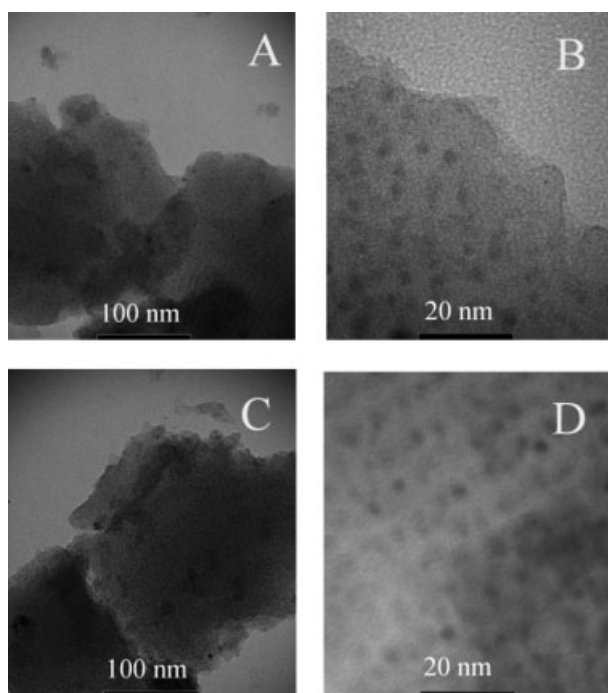


**Figure 5.** Transmission electron microscopy images of NiO/SBA-15: (a) and (b) and (c) and (d) were taken from the same areas, respectively.

the amount of adsorbed nitrogen decreases and the onset of the capillary condensation step shifts to a smaller relative pressure. The decrease of the absorption amount can be attributed to the reduced surface area, whereas the shift of inflection point of the step to lower relative pressure  $P/P_0$  is caused by the smaller pore size. The corresponding BET surface area dropped from  $893.5 \text{ m}^2 \text{ g}^{-1}$  of SBA-15 to  $329.5 \text{ m}^2 \text{ g}^{-1}$  of NiO/SBA-15, while the pore volume and pore diameter decreased from  $1.27 \text{ cc g}^{-1}$  and  $7.4 \text{ nm}$  to  $0.402 \text{ cc g}^{-1}$  and  $5.6 \text{ nm}$  respectively, which suggests that NiO may be located inside the mesopores of the host silica.

Transmission electron microscopy images (Fig. 5) give intuitive evidence on the structure of NiO/SBA-15 in which the mesoporous silica channels are well ordered and black dots of NiO particles can be identified inside the silica matrix; a particle size of  $\sim 4 \text{ nm}$  can be calculated from the magnification scale and is thus consistent with the X-ray diffraction and  $\text{N}_2$  adsorption–desorption conclusions. The high dispersion of NiO nanoparticles is ensured by the grafting reaction of  $\text{Ni}(\text{COD})_2$  upon surface silanols, which were converted into NiO nanoparticles upon thermal treatment because the strong interaction between grafted species and support to some extent prevents the aggregation of NiO during formation.

That  $\text{Ni}(\text{COD})_2$  can react with surface hydroxyl groups in the anhydrous conditions applied here is interesting for the potential of both new surface reactions and new methods to incorporate nickel(0) compounds upon the surface of

supports, but up to now little is known about the surface reaction and species formed during this process. We speculate that the hydrogen atom in surface hydroxyl groups may play an important role in the process, which may either bond directly to the cyclooctadiene ring or to the nickel metal; in both cases nickel centres are immobilized upon the surface through chemical bonding. It is also important to understand such a process because if the metals interact directly with surface hydroxyl groups, which may differ from metal to metal, especially to the less active metals, approaches to disperse isolated metal centres may be developed in this way. As such, we are continuing our research on this interesting topic.

## CONCLUSIONS

Bis(1,5-cyclooctadiene) nickel dissolved in THF can react with surface silanols of mesoporous silica under anhydrous conditions protected by argon, thus forming a strongly grafted nickel species upon silica. Afterwards, calcination of the nickel-modified mesoporous silica in air produced NiO nanoparticles inside the mesoporous silica matrix. Thermogravimetric analysis shows that the combustion of surface nickel species occurs at  $\sim 380^\circ\text{C}$  whereas both X-ray diffraction and transmission electron microscopy evidenced the formation of NiO nanoparticles inside a mesoporous matrix. Low-angle X-ray diffraction and  $\text{N}_2$  adsorption–desorption showed that the mesoporous silica structure remains intact after surface modification and NiO formation upon calcinations. The method employed here can be extended to similar systems after minor modification of the above procedures, but the grafted species after  $\text{Ni}(\text{COD})_2$  reacts with surface silanols remains unknown and is still under investigation.

## Acknowledgements

The authors would like to thank Professor Helmut Boennemann for helpful discussions. K.Z. and L.D. are grateful to the International University of Bremen for scholarship funds and R.R. also for start-up funds.

## REFERENCES

1. Zhou WZ, Thomas JM, Shephard DS, Johnson BFG, Ozkaya D, Maschmeyer T, Bell RG, Ge QF. *Science* 1998; **280**: 705.
2. Ratnasamy P, Kumar R. *Catal. Today* 1991; **9**: 329.
3. Maschmeyer T, Rey F, Sankar G, Thomas JM. *Nature* 1995; **378**: 159.
4. Zhu KK, Ma ZN, Zou Y, Zhou WZ, Chen T, He HY. *Chem. Commun.* 2001; 2552.
5. Nozaki C, Lugmair CG, Bell AT, Tilley TD. *J. Am. Chem. Soc.* 2002; **124**: 13 194.
6. Drake IJ, Furdala KL, Baxamusa S, Bell AT, Tilley TD. *J. Phys. Chem. B* 2004; **108**: 18 421.
7. Vidal V, Theolier A, Thivolle-Cazat J, Basset JM, Corker J. *J. Am. Chem. Soc.* 1996; **118**: 4595.
8. Vidal V, Theolier A, Thivolle-Cazat J, Basset JM. *Science* 1997; **276**: 99.

9. Wada K, Nakashita M, Bundo M, Ito K, Kondo T, Mitsudo T. *Chem. Lett.* 1998; 659.
10. Wada K, Yamada K, Kondo T, Mitsudo T. *Chem Lett.* 2001; 12.
11. Maxim N, Magusin PCMM, Kooyman PJ, van Wolput JHMC, van Santen RA, Abbenhuis HCL. *Chem. Mater.* 2001; **13**: 2958.
12. Maxim N, Abbenhuis HCL, Stobbelaar PJ, Mojet BL, van Santen RA. *Phys. Chem. Chem. Phys.* 1999; **1**: 4473.
13. Maxim N, Overweg A, Kooyman PJ, van Wolput JHMC, Hanssen RWJM, van Santen RA, Abbenhuis HCL. *J. Phys. Chem. B* 2002; **106**: 2203.
14. Dire S, Ceccato R, Facchin G, Carturan G. *J. Mater. Chem.* 2001; **11**: 678.
15. Thomas JM, Thomas WJ. Setting the scene. In *Principles and Practice of Heterogeneous Catalysis*. VCH: Weinheim, 1996; 1–60.
16. Boudjahem AG, Monteverdi S, Mercy M, Bettahar MM. *J. Catal.* 2004; **221**: 325.
17. Clause O, Kermarec M, Bonneviot L, Villain F, Che M. *J. Am. Chem. Soc.* 1992; **114**: 4709.
18. Che M, Cheng ZX, Louis C. *J. Am. Chem. Soc.* 1995; **117**: 2008.
19. Casula MF, Corrias A, Paschina G. *J. Mater. Res.* 2000; **15**: 2187.
20. Zhao DY, Feng JL, Huo QS, Melosh N, Fredrickson GH, Chemlka BF, Stucky GD. *Science* 1998; **279**: 548.